

High-Performance Transistor Based on Individual Single-Crystalline Micrometer Wire of Perylo[1,12-*b,c,d*]thiophene

Yanming Sun,[†] Lin Tan,[†] Shidong Jiang,[‡] Hualei Qian,[†] Zhaohui Wang,^{*,†} Dongwei Yan,[§] Chongan Di,[†] Ying Wang,[†] Weiping Wu,[†] Gui Yu,[†] Shouke Yan,[‡] Chunru Wang,[§] Wenping Hu,[†] Yunqi Liu,^{*,†} and Daoben Zhu^{*,†}

Beijing National Laboratory for Molecular Sciences, Key Laboratory of Organic Solids, State Key Laboratory of Polymer Physics and Chemistry, and Key Laboratory of Molecular Nanostructure and Nanotechnology, Institute of Chemistry, Chinese Academy of Sciences, Beijing 100080, China

Received November 11, 2006; E-mail: wangzhaohui@iccas.ac.cn; liuyq@mail.iccas.ac.cn

Over the past 20 years, organic field-effect transistors (OFETs) based on soluble polymers and conjugated oligomers have attracted enormous interest for the realization of organic electronic devices.¹ Pentacene as the benchmark material with a mobility beyond $1.0 \text{ cm}^2 \text{ V}^{-1} \text{ s}^{-1}$ has been reported.² Despite the great progress in the exploration of functional organic materials for OFETs,³ fundamental aspects of carrier transport, especially the role of solid-state packing, still remain unclear.⁴ From the standpoint of bandwidth and the hopping theory of carrier conduction, a cofacial π stacking structure is expected to facilitate carrier transport.^{4,5} However, most of the organic semiconductors with high mobilities have a herringbone structure which reduces the overlap.⁶ On the other hand, the research work for OFETs has mainly focused on thin-film and bulk single-crystal state. Study of micro- and nanomaterials, including fibers, ribbons, and wires, has only been recently reported because of the potential applications in integrated (opto) electronic devices due to many unique properties, such as flexibility, high photoconductivity, and nonlinear optical effects, etc.⁷ Herein we present our studies of a new class of a high-performance OFET semiconductor based on perylo[1,12-*b,c,d*]thiophene (PET, Figure 1). The integration of a S atom into the polycyclic aromatic hydrocarbon (PAH) skeleton induces an extraordinary solid-state packing arrangement with the likelihood of double-channel superstructure, which is expected to permit effective charge transporting. Furthermore, we have grown its micrometer single-crystal wires by physical vapor transport and successfully applied them to transistors. The devices exhibit excellent performance with a high mobility up to $0.8 \text{ cm}^2 \text{ V}^{-1} \text{ s}^{-1}$.

The oligothiophene and PAHs are among the most versatile and effective molecular scaffolds for organic functional materials. It is thus surprising that little effort has been devoted to exploiting sulfur heterocyclic PAHs in OFETs. We choose PET as an ideal system for investigating structure–property relationships among organic semiconductors because of its unique packing in single crystals (Figure 1). Although its synthesis was first reported by Rogovik,⁸ its electrical property is rarely studied. The crystal structure contains almost planar PET molecules stacked along the *b*-axis with interplanar distances of 3.47 \AA ,⁹ in contrast to the sandwich herringbone packing of perylene crystals. Remarkably, marked S \cdots S short contacts (3.51 \AA) were found between the neighboring columns related by an inversion center. The double-channel fashion is envisioned to be transformed into the facile establishment of a high-performance charge transport system.

As a control result, we have first investigated the thin-film field-effect behavior of PET. Transistors have been fabricated on SiO_2 /

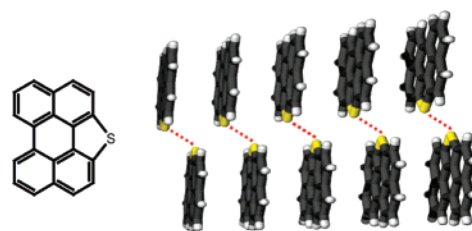


Figure 1. Chemical structure and crystal packing view of PET.

Si substrate with octadecyltrichlorosilane (OTS) treatment, adopting a top-contact configuration. Only *p*-channel activity is observed for the device. It exhibits a good linear and saturated curve. From the transfer curve (Supporting Information, Figure S2), a moderate mobility of $0.05 \text{ cm}^2 \text{ V}^{-1} \text{ s}^{-1}$, an on/off ratio about 1.2×10^5 , a threshold voltage of -6.3 V , and a subthreshold swing of 4 V per decade have been obtained.

We used scanning electron microscopy (SEM) and X-ray diffraction measurement (XRD) to elucidate the structures of PET. The images of thin films deposited on SiO_2/Si at room temperature are shown in Figure S3. Homogeneous strips consist of the thin films with the average length and width of about $2 \text{ }\mu\text{m}$ and 300 nm , respectively. Highly crystalline films were observed for thin films of PET (Figure S4). XRD profiles indicate a first diffraction peak at $2\theta = 5.32^\circ$ (*d* spacing 16.6 \AA) with the second-order diffraction peak at $2\theta = 10.64^\circ$ (*d* spacing 8.3 \AA) and fourth order diffraction peak at $2\theta = 21.3^\circ$ (*d* spacing 4.13 \AA). The first diffraction peak of PET is assigned as (001) and the remaining higher order peaks as (00*l*). The multiple orders of reflection, consistent with a single preferred orientation, indicate the films are well-ordered, layered microstructures. The 16.6 \AA (*d* spacing) determined by XRD measurements is about twice the value of molecular length, which suggests that the molecules are oriented with their long axis almost normal to the film and the π – π stacking direction parallel to the substrate. In this configuration, the charge carriers would transport easily.

During the growth of a PET single crystal, we found that the PET molecules easily assembled into wires. Consequently, micrometer wires have been grown directly on SiO_2 with OTS treatment by physical vapor transport method by adjusting the temperature and time. OTS was used to form a siloxane self-assembled monolayer (SAM) on the SiO_2 layer, which could promote and facilitate molecular self-organization of compounds during the deposition.¹⁰ The detail for fabrication is described in the Supporting Information. Figure 2A displays the images of the large-area PET micrometer-sized wires, whose diameter is in the range of $1\text{--}2 \text{ }\mu\text{m}$, while the length can be hundreds of micrometers. Bright field transmission electron microscopic (TEM) observations,

[†] Key Laboratory of Organic Solids.

[‡] State Key Laboratory of Polymer Physics and Chemistry.

[§] Key Laboratory of Molecular Nanostructure and Nanotechnology.

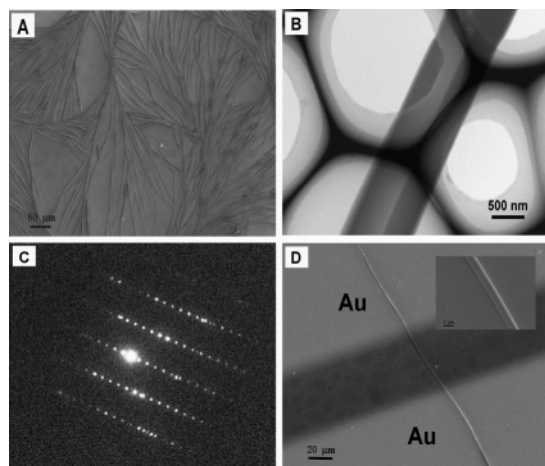


Figure 2. (A) Images of the large-area PET micrometer-sized wires grown directly on the SiO₂/Si substrate with OTS treatment. (B) TEM image of a single-crystal PET wire, and (C) its corresponding electron diffraction pattern. (D) Micrograph of an individual PET wire and the electrodes formed by a gold wire mask. Inset: The magnification image of the individual PET wire between the two electrodes.

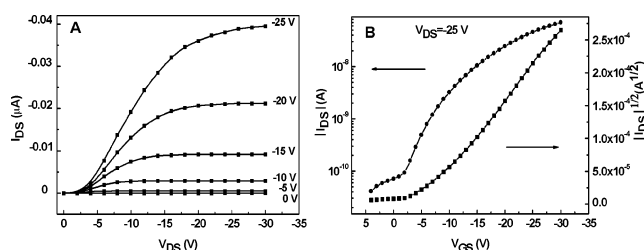


Figure 3. The electrical characteristics of the transistor based on individual micrometer PET wire: (A) output curve, (B) transfer characteristics of the device.

see Figure 2B as an example, demonstrate that the wires exhibit regular rectangular shapes. The corresponding electron diffraction pattern (Figure 2c) shows sharp and well-defined reflection spots, which are all accounted for the monoclinic unit cell with axes $a = 16.921$, $b = 4.5252$, $c = 17.898$ Å, and $\beta = 112.655^\circ$ as the $(0kl)$ reflections. This indicates that the wires exhibit single-crystal structures. The electron diffraction result further indicates that the long axis of the rectangular single crystal is along the b -axis.

It is well-known that the single crystals of organic semiconductors could eliminate the existence of disorder and grain boundaries in thin films and lead to higher mobilities. Consequently, transistors based on an individual wire of PET have been fabricated by evaporating a thin layer of Au onto the wire supported by the SiO₂/Si substrate at a vacuum pressure of 1.0×10^{-3} Pa with a gold wire as mask. As seen in Figure 2D, the length of the wire between the electrodes is $55 \mu\text{m}$ and its width is $1.8 \mu\text{m}$. The electrical characteristics are shown in Figure 3. The transistor exhibits p -channel behavior with a mobility of $0.8 \text{ cm}^2 \text{ V}^{-1} \text{ s}^{-1}$, a low threshold voltage of -6.0 V, and an on/off ratio of 1.7×10^3 . Figure 3A shows the output curve of the transistor. It can be seen, at a low drain voltage, that the current is at off state, indicative of the presence of contact resistance.^{7c,11} Therefore, optimizing the fabrications of the devices may lead to further improvements of the transistor performance. The mobilities were measured to be in the range of 0.3 – $0.8 \text{ cm}^2 \text{ V}^{-1} \text{ s}^{-1}$ for the fabricated six transistors, which is higher than that of the perylene single-crystal transistor.¹²

The strong S...S interactions of the molecules may contribute to the high performance. Furthermore, we performed a shelf-life test for one transistor under ambient conditions; the mobility only varied from 0.35 to $0.34 \text{ cm}^2 \text{ V}^{-1} \text{ s}^{-1}$, and the on/off ratio was almost unchanged after about 1 week, indicating good stability of the devices.

In conclusion, we have investigated the thin-film field-effect behavior of PET, which exhibits a moderate mobility of $0.05 \text{ cm}^2 \text{ V}^{-1} \text{ s}^{-1}$, an on/off ratio of 10^5 , and a low threshold voltage of -6.3 V at room temperature. Moreover, we have grown its single-crystal micrometer wires and successfully applied them to transistors. A mobility up to $0.8 \text{ cm}^2 \text{ V}^{-1} \text{ s}^{-1}$, a low threshold voltage of -6.0 V, and an on/off ratio of 1.7×10^3 could be achieved. The extraordinary solid-state packing arrangement with the likelihood of double-channel fashion induced by marked S...S interactions may contribute to the high performance.

Acknowledgment. The authors would like to acknowledge financial support from the National Natural Science Foundation of China (20472089, 90206049, 20421101, 50673093, 20573115, 20642001, 60671047), 973 Program (2006CB806200, 2006CB932100), and Chinese Academy of Sciences.

Supporting Information Available: Details of experimental procedures, additional data or spectra, information of device fabrication and growth of PET micrometer wires. This material is available free of charge via the Internet at <http://pubs.acs.org>.

References

- (a) Dimitrakopoulos, C. D.; Malenfant, P. R. L. *Adv. Mater.* **2002**, *14*, 99. (b) Katz, H. E. *Chem. Mater.* **2004**, *16*, 4748. (c) Sirringhaus, H. *Adv. Mater.* **2005**, *17*, 2411. (d) Newman, C. R.; Frisbie, C. D.; da Silva Filho, D. A.; Bredas, J.-L.; Ewbank, P. C.; Mann, K. R. *Chem. Mater.* **2004**, *16*, 4436. (e) Facchetti, A.; Yoon, M. H.; Marks, T. J. *Adv. Mater.* **2005**, *17*, 1705. (f) Reese, C.; Bao, Z. *J. Mater. Chem.* **2006**, *16*, 329. (g) Sun, Y.; Liu, Y.; Zhu, D. *J. Mater. Chem.* **2005**, *15*, 53.
- (a) Lin, Y.-Y.; Gundlach, D. J.; Nelson, S. F.; Jackson, T. N. *IEEE Electron Device Lett.* **1997**, *18*, 606. (b) Klauk, H.; Halik, M.; Zschieschang, U.; Schmid, G.; Radlik, W.; Weber, W. *J. Appl. Phys.* **2002**, *92*, 5259.
- (a) Sundar, V. C.; Zaumseil, J.; Podzorov, V.; Menard, E.; Willett, R. L.; Someya, T.; Gershenson, M. E.; Rogers, J. A. *Science* **2004**, *303*, 1644. (b) Meng, H.; Sun, F.; Goldfinger, M. B.; Gao, F.; Londono, D. J.; Marshall, W. J.; Blackman, G. S.; Dobbs, K. D.; Keys, D. E. *J. Am. Chem. Soc.* **2006**, *128*, 9304. (c) Wu, Y.; Li, Y.; Gardner, S.; Ong, B. S. *J. Am. Chem. Soc.* **2005**, *127*, 614. (d) Yoon, M. H.; DiBenedetto, S. A.; Facchetti, A.; Marks, T. J. *J. Am. Chem. Soc.* **2005**, *127*, 1348. (e) Xiao, K.; Liu, Y.; Qi, T.; Zhang, W.; Wang, F.; Gao, J.; Qiu, W.; Ma, Y.; Cui, G.; Chen, S.; Zhan, X.; Yu, G.; Qin, J.; Hu, W.; Zhu, D. *J. Am. Chem. Soc.* **2005**, *127*, 13281. (f) Sun, Y. M.; Ma, Y. Q.; Liu, Y. Q.; Lin, Y. Y.; Wang, Z. Y.; Wang, Y.; Di, C. A.; Xiao, K.; Chen, X. M.; Qiu, W. F.; Zhang, B.; Yu, G.; Hu, W. P.; Zhu, D. B. *Adv. Funct. Mater.* **2006**, *16*, 426. (g) Meng, H.; Sun, F.; Goldfinger, M. B.; Jaycox, G. D.; Li, Z.; Marshall, W. J.; Blackman, G. S. *J. Am. Chem. Soc.* **2005**, *127*, 2406. (h) Payne, M. M.; Parkin, S. R.; Anthony, J. E.; Kuo, C.-C.; Jackson, T. N. *J. Am. Chem. Soc.* **2005**, *127*, 4986. (i) Takimiya, K.; Kunugi, Y.; Konda, Y.; Ebata, H.; Toyoshima, Y.; Otsubo, T. *J. Am. Chem. Soc.* **2006**, *128*, 3044.
- Moon, H.; Zeis, R.; Borkent, E. J.; Besnard, C.; Lovinger, A. J.; Siegrist, T.; Kloc, C.; Bao, Z. *J. Am. Chem. Soc.* **2004**, *126*, 15322.
- Brédas, J. L.; Calbert, J. P.; da Silva Filho, D. A.; Cornil, J. *Proc. Natl. Acad. Sci. U.S.A.* **2002**, *99*, 5804.
- Curtis, M. D.; Cao, J.; Kampf, J. W. *J. Am. Chem. Soc.* **2004**, *126*, 4318.
- (a) Kim, D. H.; Han, J. T.; Park, Y. D.; Jang, Y.; Cho, J. H.; Hwang, M.; Cho, K. *Adv. Mater.* **2006**, *18*, 719. (b) Tang, Q.; Li, H.; He, M.; Hu, W.; Liu, C.; Chen, K.; Wang, C.; Liu, Y.; Zhu, D. *Adv. Mater.* **2006**, *18*, 65. (c) Xiao, S.; Tang, J.; Beetz, T.; Guo, X.; Tremblay, N.; Siegrist, T.; Zhu, Y.; Steigerwald, M.; Nuckolls, C. *J. Am. Chem. Soc.* **2006**, *128*, 10700.
- Rogovik, V. I. *J. Org. Chem. (USSR)* **1974**, *10*, 1072.
- Santos, I. C.; Almeida, M.; Morgado, J.; Duarte, M. T.; Alcácer, L. *Acta Crystallogr.* **1997**, *C53*, 1640.
- (a) Shtein, M.; Mapel, J.; Benziger, J. B.; Forrest, S. R. *Appl. Phys. Lett.* **2002**, *81*, 268. (b) Gundlach, D. J.; Nichols, J. A.; Zhou, L.; Jackson, T. N. *Appl. Phys. Lett.* **2002**, *80*, 2925.
- Wu, Y.; Li, Y.; Ong, B. S. *J. Am. Chem. Soc.* **2006**, *128*, 4202.
- Kotani, M.; Kakinuma, K.; Yoshimura, M.; Ishii, K.; Yamazaki, S.; Kobori, T.; Okuyama, H.; Kobayashi, H.; Tada, H. *Chem. Phys.* **2006**, *325*, 160.

JA068079G